anisotropy will produce a potentially large uncertainty in the magnitude of the Kerr constant but not its sign. Thus, a difference by a factor of 3 or 4 in the magnitude of experimental and calculated values of the Kerr constant is not surprising or even distressing. It is interesting to note that large positive Kerr constants of the ethyl and methyl derivatives (Table III) require the skew-trapezoidal-bipyramidal geometry and rule out the cis configuration entirely for those structures.

Registry No. *trans*-$(C_4H_9)Sn(dbzm)_2$, 22673-17-2; *skew*-$(C_2H_5)_2Sn(dbzm)_2$, 60828-32-2; *skew*-$(CH_3)_2Sn(dbzm)_2$, 53319-86-1; *cis*-$(CH_3)_2Sn(OX)_2$, 20347-45-9; *trans*-$(C_2H_5)_2Sn(Trop)_2$, 21729-19-1; *cis*-$(C_2H_5)_2Sn(dbzm)_2$, 60828-31-1.

Contribution from the Department of Chemistry,
The University of Mississippi, University, Mississippi 38677

Electrochemical Studies of Chloro Complex Formation in Low-Temperature Chloroaluminate Melts. 1. Iron(II), Iron(III), and Nickel(II)

T. M. LAHER and G. L. HUSSEY*

Received February 17, 1982

A potentiometric titration procedure was used to study the coordination of iron(II) and iron(III) in the aluminum chloride–*N*-*n*-butylpyridinium chloride ($AlCl_3$–BPC) melt containing excess chloride ion (basic melt). Potentiometric measurements on the cells Al|$AlCl_3$–BPC (66.7:33.3 mol %)|fritted disk|$AlCl_3$–BPC, $Fe(II)_{dil}$|Fe and Al|$AlCl_3$–BPC (66.7:33.3 mol %)|fritted disk|$AlCl_3$–BPC, $Fe(II)_{dil}$, $Fe(III)_{dil}$|Pt were made while the ratio of $AlCl_3$ to BPC was varied in the right-hand cell compartment. Analysis of the data obtained indicated that iron(II) and iron(III) are complexed as $FeCl_4^{2-}$ and $FeCl_4^-$, respectively, in basic melt. Similar potentiometric titration data for the Fe(III)/Fe(II) couple in $AlCl_3$-rich (acidic) melt were consistent with a two-chloride-ion dependence. Average stoichiometric formation constants for $FeCl_4^{2-}$ and $FeCl_4^-$ were found to be 5.0×10^{46} and 7.9×10^{77}, respectively. The formation constant for $NiCl_4^{2-}$, redetermined in the present study, was 5.0×10^{49}, referenced to the 66.7:33.3 mol % melt.

Introduction

Mixtures of aluminum chloride and certain *N*-alkylpyridinium halides form molten salts that are liquid at or close to room temperature. One of these systems, aluminum chloride–*N*-*n*-butylpyridinium chloride ($AlCl_3$–BPC), is liquid at 27 °C over a composition range that includes mixtures containing from 66.7 to 44.0 mol % $AlCl_3$.[1] Potentiometric studies indicate that the distribution of chloroaluminate species in the $AlCl_3$–BPC melt can be expressed by means of a single equilibrium reaction[2]

$$2AlCl_4^- \rightleftharpoons Al_2Cl_7^- + Cl^- \tag{1}$$

with a value of $K = 1.2 \times 10^{-13}$ at 40 °C.[3] The variation in $AlCl_3$ content possible in this melt system permits substantial changes in melt chloride ion activity to be made at relatively low liquidus temperatures.

Previous investigations involving nickel(II)[4] and cobalt(II)[5] indicated that the basic (BPC-rich) $AlCl_3$–BPC melt is an interesting, anhydrous, ionic solvent in which to study the coordination of transition-metal ions by chloride ion. For example, Gale et al.[4] reported that nickel(II) exists in the form of a very stable, tetrahedral $NiCl_4^{2-}$ species in this melt composition region. Similarly, cobalt(II) was complexed as a tetrahedral $CoCl_4^{2-}$ species in basic $AlCl_3$–BPC melt.[5] The stoichiometric formation constant, based on ion mole fractions, for $CoCl_4^{2-}$ in an $AlCl_3$–BPC melt was considerably larger than values obtained in inorganic chloroaluminate melts.[5]

In the present study iron(II) and iron(III) chloro complex formation was examined in the basic $AlCl_3$–BPC melt. This study was undertaken as part of a continuing investigation of the nature and energetics of the coordination of transition-metal ions by melt chloride ion in the low-melting chloroaluminate melt system, $AlCl_3$–BPC. Additional data concerning formation of $NiCl_4^{2-}$ were also obtained in this study.

Experimental Section

All experiments were conducted in a dry, oxygen-free nitrogen atmosphere inside a Kewaunee Scientific Equipment Corp. drybox equipped with a 3-cfm inert-gas purifier. The quality of the atmosphere inside the drybox was tested daily by observing the lifetime of a lighted 25-W light bulb with a hole pierced in its glass envelope. The drybox atmosphere was found acceptable when the bulb remained lighted for 2 h or more.

Potentiometric titration experiments were carried out in a Pyrex H-cell. One side arm of this cell served as the working compartment and had a total volume of about 10 mL. Melt solution in this compartment was stirred continuously by means of a miniature Teflon-covered stirbar and magnetic stirrer. The other side arm was used as the reference compartment. The working and reference compartments of the cell were separated from one another by a center compartment with 10-mm fine porosity fritted disks at each end. The porous areas of both fritted disks were decreased substantially by heating them strongly in the flame of a glass-blowing torch. This greatly reduced leakage between compartments but permitted electrical contact. The center compartment of the cell was filled with melt through a small side arm.

The temperature of the cell was maintained at 40 ± 0.2 °C in a furnace machined from a massive aluminum block. The furnace was heated by two 150-W Vulcan Electric cartridges. Regulated current to power the furnace was provided by an Ace Glass temperature controller equipped with a thermistor sensor. The temperature of the cell was monitored by means of a glass-sheathed chromel–alumel thermocouple connected to a Model 410A Doric Trendicator. Potentials were measured with a Keithley Model 178 digital multimeter. The cell and instrumentation used to coulometrically generate metal ions in the melt and to perform cyclic voltammetry were identical with those described previously.[5]

Anhydrous $AlCl_3$ (Fluka, A.G.) was sublimed under vacuum directly inside the drybox a minimum of three times. The preparation and purification of BPC are detailed in a previous publication.[6] For

---

[1] Robinson, J.; Osteryoung, R. A. *J. Am. Chem. Soc.* **1979**, *101*, 323.
[2] Gale, R. J.; Osteryoung, R. A. *Inorg. Chem.* **1979**, *18*, 1603.
[3] Schoebrechts, J. P.; Gilbert, B. P. *J. Electrochem. Soc.* **1981**, *128*, 2679.
[4] Gale, R. J.; Gilbert, B.; Osteryoung, R. A. *Inorg. Chem.* **1979**, *18*, 2723.
[5] Hussey, C. L.; Laher, T. M. *Inorg. Chem.* **1981**, *20*, 4201.
[6] Carpio, R. A.; King, L. A.; Lindstrom, R. E.; Nardi, J. C.; Hussey, C. L. *J. Electrochem. Soc.* **1979**, *126*, 1644.

0020-1669/82/1321-4079$01.25/0

brevity, the melt compositions specified throughout this paper will be expressed in terms of the mole percent (mol %) of $AlCl_3$ in each $AlCl_3$–BPC mixture. Aluminum wire (Alfa Products, m5N) was etched in an aqueous solution containing 5% HF and 15% HNO_3 by volume, rinsed with distilled water, and dried under vacuum prior to use. Anhydrous $FeCl_3$ (Alfa Products, 98%) was used as received. Iron electrodes were fashioned from lengths of 2-mm diameter iron wire (Johnson Matthey Chemicals, Puratronic grade). They were polished with emery cloth, washed with acetone, and dried with Kimwipes inside the drybox before use. Nickel electrodes were constructed from Marz grade nickel foil (Materials Research Corp.) and were treated in a fashion similar to that for the iron electrodes prior to use. Both iron(II) and nickel(II) were introduced into the melt coulometrically to avoid experimental difficulties associated with the handling of $FeCl_2$ and $NiCl_2$. However, no chemical or electrochemical difference could be discerned between solutions prepared by coulometric addition of iron(II) or nickel(II) and those prepared by addition of anhydrous $FeCl_2$ or $NiCl_2$, respectively.

Results and Discussion

Potentiometric Titration Measurements. The number of chloride ligands associated with iron(II) in a BPC-rich melt and an estimate of the stoichiometric formation constant for its chloro complex were calculated from potentiometric titration data obtained with the cell arrangement depicted for cell I. A similar cell was used for reexamination of nickel(II)

$$Al|AlCl_3\text{–BPC}(66.7:33.3\ \text{mol}\ \%)|\text{fritted disk}|AlCl_3\text{–BPC},\ Fe(II)_{dil}|Fe \quad (I)$$

chloro complex formation, except that dilute nickel(II) was introduced into the right-hand cell compartment instead of iron(II) and the iron electrode was replaced by a nickel electrode. A cell of slightly different construction, equipped with a platinum indicator electrode, was used to study iron(III) chloro complex formation (cell II).

$$Al|AlCl_3\text{–BPC}(66.7:33.3\ \text{mol}\ \%)|\text{fritted disk}|AlCl_3\text{–BPC},\ Fe(III)_{dil},\ Fe(II)_{dil}|Pt \quad (II)$$

Potential measurements were made on these cells as a function of the amount of BPC relative to $AlCl_3$ in the right-hand cell compartment. The composition of melt in the left-hand compartment was kept constant, since it served as the reference half-cell. Cell potentials were generally stable to within ±0.005 V and well-behaved throughout an individual titration. However, maximum deviation between experimental titration curves, acquired under identical conditions with equivalent cells, electrodes, and melt, was ca. ±0.050 V. An accurate estimate of the initial composition of each melt used in the right-hand cell compartment was determined from the equivalence point of the titration curve. Due to difficulties in preparing melts that were exactly 66.7 mol % in $AlCl_3$ at the outset of each titration experiment, some melts were used that contained slightly less $AlCl_3$, e.g., 66.2 mol % $AlCl_3$. Apparent standard potential values measured in these melts were corrected to melt containing 66.7 mol % $AlCl_3$ to ensure that each formation constant calculation was referenced to the same melt composition. When necessary, correction factors were estimated from an extrapolation of the initial portion of the titration curve associated with each apparent standard potential determination. The difference in potential between the initial point on the titration curve (before BPC was added) and a point obtained by extrapolating the completing curve to the 66.7 mol % composition was added to the apparent standard potential value. These corrections were 0.060 V or less.

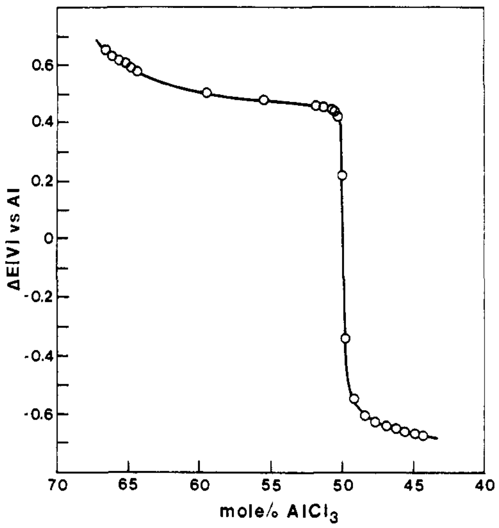

Figure 1. Potentiometric titration curve for titration of iron(II) in $AlCl_3$–BPC at 40.0 °C. The initial iron(II) concentration was 4.32×10^{-3} M. The melt was 66.7 mol % in $AlCl_3$ prior to the outset of the titration.

Iron(II). The data resulting from potentiometric titration of iron(II) in $AlCl_3$–BPC melt are shown in Figure 1. The initial iron(II) concentration was 4.32×10^{-3} M. The iron(II) was introduced into the melt by coulometric dissolution of an iron wire potentiostated at 1.4 V. Insolubility of the iron(II) species was noted during the titration when the melt was ca. 50.0 mol % in $AlCl_3$. The precipitate was identical in appearance with $FeCl_2$. The insolubility of other metal species, e.g., $CoCl_2$[5,7-9] and UCl_3,[10] in equimolar chloroaluminate melts has been reported. Solutions of iron(II) in acidic melt (>50 mol % in $AlCl_3$) were almost colorless, while iron(II) solutions prepared with basic melt were pale yellow.

If iron(II) forms essentially a single mononuclear chloro complex in the basic melt region examined, analogous to the case for nickel(II)[4] and cobalt(II)[5] in $AlCl_3$–BPC, then the potential of the cell depicted in (I) should vary with melt chloride ion activity according to the Nernst equation for the half-cell reaction

$$FeCl_p^{2-p} + 2e^- \rightleftharpoons Fe + pCl^- \qquad (2)$$

A plot of the cell potential, ΔE, vs. log X_{Cl^-}, where X_{Cl^-} is the calculated chloride ion mole fraction, was constructed for the data shown in Figure 1 that appear in the composition interval extending from ca. 49.0 to 44.3 mol % $AlCl_3$. This graph was linear and exhibited a slope of 0.128 ± 0.001 V. A value of $p = 4.1$ for eq 2 was calculated from this slope. The linearity of this graph and the estimate obtained for p suggest that $FeCl_4^{2-}$ is the sole iron(II) chloro complex formed in the melt composition interval described above and that the activity coefficient for melt chloride ion in BPC-rich melt is constant over the range of mole fractions investigated.

The formation of $FeCl_4^{2-}$ in basic melt is consistent with data reported for iron(II) coordination in other anhydrous molten salts containing ionic chloride. For example, Gruen and McBeth[11] interpreted the spectrum of iron(II) in molten LiCl–KCl in terms of tetrahedral and distorted-tetrahedral $FeCl_4^{2-}$. Deviations from ideality in the system $FeCl_2$–KCl at 1000 °C, determined via activity measurements with the cell $Fe|FeCl_2, KCl|C, H_2, HCl$ implied formation of $FeCl_4^{2-}$.[12] In contrast, iron(II) in molten molecular Al_2Cl_6 is reported to exhibit octahedral coordination by chloride bound to aluminum via two $Al_2Cl_7^-$ ions associated with each iron(II) ion.[13]

---

(7) Øye, H. A.; Gruen, D. M. *Inorg. Chem.* **1965**, *4*, 1173.
(8) Kvaal, T.; Øye, H. A. *Acta Chem. Scand.* **1972**, *26*, 1647.
(9) Nikolic, R.; Øye, H. A. *Z. Phys. Chem.* (*Leipzig*) **1979**, *260*, 841.
(10) Moore, R. H. *Inorg. Chem.* **1964**, *3*, 1738.
(11) Gruen, D. M.; McBeth, R. L. *Pure Appl. Chem.* **1963**, *6*, 23.
(12) Ernst, W.; Flood, H.; Nervik, T. *Z. Anorg. Allg. Chem.* **1968**, *363*, 89.
(13) Øye, H. A.; Gruen, D. M. *Inorg. Chem.* **1964**, *3*, 836.

Table I. Potentials, Ion Mole Fractions, and Calculated Stoichiometric Formation Constants for $FeCl_4^{2-}$

E, V	X_{AlCl_3}[a]	$10^2X_{Cl^-}$[b]	$10^4X_{FeCl_4^{2-}}$	$10^2X_{Cl^-}$[c]	log $\beta'_{FeCl_4^{2-}}$
−0.605	0.484	3.11	3.33	2.98	46.1
−0.624	0.477	4.44	3.24	4.32	46.2
−0.639	0.469	5.80	3.14	5.68	46.2
−0.649	0.462	7.04	3.05	6.92	46.1
−0.658	0.456	8.12	2.97	8.00	46.2
−0.665	0.449	9.24	2.89	9.13	46.2
−0.671	0.443	10.25	2.82	10.14	46.2

[a] Apparent mole fraction of $AlCl_3$, excluding chloroaluminate ion formation. [b] Chloride ion mole fraction in excess of the 50.0 mol % $AlCl_3$–BPC melt composition. [c] Excess chloride ion less the amount complexed as $FeCl_4^{2-}$.

The stoichiometric formation constant for $FeCl_4^{2-}$, based on ion mole fractions, $\beta'_{FeCl_4^{2-}}$, can be estimated for each value of ΔE and log X_{Cl^-} in the basic melt by means of the expression

$$\Delta E = E^{\circ\prime}_{Fe(II)/Fe} + 2.3(RT/2F)\log X_{FeCl_4^{2-}} - 2.3(RT/2F)\log \beta'_{FeCl_4^{2-}} - 2.3(RT/2F)\log X_{Cl^-}{}^4 + E_j \quad (3)$$

In this equation $E^{\circ\prime}_{Fe(II)/Fe}$ is the apparent standard potential for Fe(II) on the mole fraction scale in 66.7 mol % melt, $X_{FeCl_4^{2-}}$ is the $FeCl_4^{2-}$ ion mole fraction, and E_j is the cell liquid junction potential. (It was necessary to derive eq 3, 5, and 7 in approximate forms employing ion mole fractions rather than activities, since activity coefficients for the various species involved are not known.) The 66.7 mol % melt was chosen as the reference point for these calculations because the chloride ion activity in this melt is the lowest that can be obtained under practical experimental conditions.[2,3] The sole anionic constituent of this melt is reported to be $Al_2Cl_7^-$.[14]

A value of $E^{\circ\prime}_{Fe(II)/Fe} = 0.773 \pm 0.016$ V was determined from the intercepts of linear Nernst plots constructed from data obtained by coulometric generation of iron(II) in a melt of appropriate composition. The slopes of these plots were 0.031 ± 0.000 V. The linearity of these plots suggests that the activity coefficient for iron(II) does not vary appreciably with iron(II) concentration. The formal concentration of iron(II) in the melt was used to calculate $X_{FeCl_4^{2-}}$ on the assumption that $\beta'_{FeCl_4^{2-}}$ is large. This assumption was found to be correct (vide infra). At the present time there is no information available about the external transport numbers of the various charge-carrying species present in the $AlCl_3$–BPC melt with which to directly calculate E_j. However, E_j values, estimated for cells similar in construction to those examined in the present study,[3] were well within the experimental error of our measurements. Thus, E_j was assumed small and ignored in this and subsequent calculations. The experimentally observed potentials, various ion mole fractions, and calculated $\beta'_{FeCl_4^{2-}}$ values obtained during a titration experiment involving iron(II) are collected in Table I. The $\beta'_{FeCl_4^{2-}}$ values that appear in this table were corrected for the amount of chloride ion complexed by iron(II).

Iron(II) and several closely related dipositive 3d ions are known to be octahedrally coordinated in molten Al_2Cl_6[13] and aluminum chloride rich chloroaluminate melts.[5,7-9] Similar observations have been reported for titanium(III) in molten Al_2Cl_6 and very acidic $AlCl_3$–KCl melt.[15] At the present time the nature of the coordination of iron(II) in the 66.7% $AlCl_3$–BPC melt is uncertain. It was not possible to obtain a useful UV–vis absorption spectrum of iron(II) in this melt, due to solubility limitations. However, if iron(II) is not directly bound to chloride in this melt, then the $\beta'_{FeCl_4^{2-}}$ values that are given in Table I represent the product of the stoichiometric stepwise formation constants $K_1'K_2'K_3'K_4'$. Likewise, if iron(II) is directly bound to one chloride ion in this melt, resulting in the formation of a species like $FeCl^+$ solvated or complexed by chloroaluminate species, the parametric formation of eq 3 does not change but $\beta'_{FeCl_4^{2-}}$ values, calculated by using this equation, would represent $K_2'K_3'K_4'$. However, $\beta'_{FeCl_4^{2-}}$ can still be functionally defined as the overall stability constant for $FeCl_4^{2-}$.

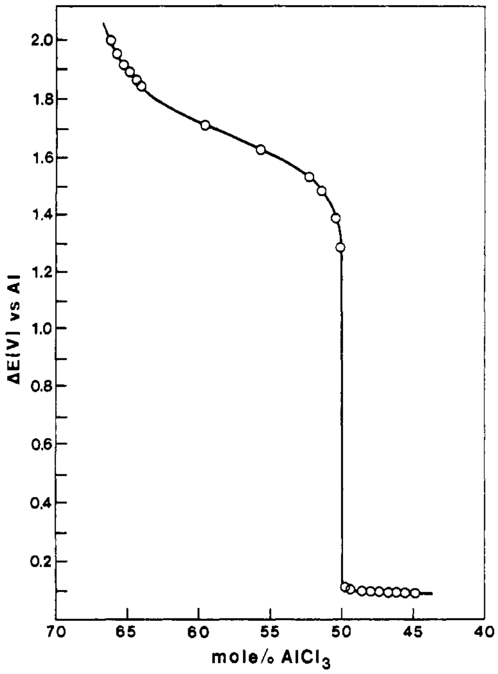

Figure 2. Potentiometric titration curve for titration of an equimolar mixture of iron(III) and iron(II) in $AlCl_3$–BPC at 40.0 °C. The initial concentrations of iron(III) and iron(II) were 1.26×10^{-3} M. The melt was 66.1 mol % in $AlCl_3$ prior to the outset of the titration.

Iron(III). A representative potentiometric titration curve for an equimolar mixture of iron(III) and iron(II) is shown in Figure 2. The iron(III) was introduced into the melt as $FeCl_3$ and exactly half of the added iron(III) was coulometrically reduced to iron(II) in a glassy carbon crucible. This was done immediately after introduction of the $FeCl_3$, since iron(III) appears to slowly oxidize the 66.7 mol % melt.[16] An equimolar mixture of iron(III) and iron(II) in this melt was stable. If iron(III) forms a mononuclear chloro complex in BPC-rich melt similar to that observed for iron(II), then ΔE for the cell depicted in (II) should vary with X_{Cl^-} in a manner consistent with the Nernst equation for the half-cell reaction

$$FeCl_q{}^{3-q} + e^- \rightleftharpoons FeCl_4{}^{2-} + (4 - q)Cl^- \quad (4)$$

Examination of Figure 2 reveals that ΔE varied very little when the $AlCl_3$ content in the right-hand cell compartment was changed from 49.4 to about 44.9 mol % $AlCl_3$. The slope of a plot of ΔE vs. log X_{Cl^-}, calculated for this composition interval, was small, ca. 0.014 ± 0.001 V. A value of $q = 3.8$, consistent with the formation of $FeCl_4^-$, was calculated from this slope. A cyclic voltammogram for iron(III) in 44.4 mol % melt at 40 °C was identical with a voltammogram for iron(III) in the nominal 50 mol % melt reported in a previous study.[16] Analysis of the former voltammogram indicated that it too corresponds to a single, one-electron reversible redox process. This suggests that only one reducible iron(III) species, $FeCl_4^-$, and one oxidizable iron(II) species, $FeCl_4^{2-}$ (vide su-

---

[14] Gale, R. J.; Gilbert, B.; Osteryoung, R. A. *Inorg. Chem.* **1978**, *17*, 2728.

[15] Sørlie, M.; Øye, H. A. *Inorg. Chem.* **1981**, *20*, 1384.

[16] Hussey, C. L.; King, L. A.; Wilkes, J. S. *J. Electroanal. Chem. Interfacial Electrochem.* **1979**, *102*, 321.

Table II. Potentials, Ion Mole Fractions, and Calculated Stoichiometric Formation Constants for $FeCl_4^-$

E, V	X_{AlCl_3}[a]	$10^2 X_{Cl^-}$[b]	$10^5 X_{FeCl_4^-}$[c]	$10^2 X_{Cl^-}$[d]	log $\beta'_{FeCl_4^-}$
0.100	0.486	2.68	9.84	2.62	77.8
0.099	0.480	3.89	9.59	3.84	77.8
0.098	0.474	5.01	9.36	4.96	77.8
0.097	0.468	6.07	9.14	6.02	77.8
0.095	0.462	7.13	8.92	7.08	77.8
0.094	0.456	8.13	8.71	8.08	77.9
0.093	0.450	9.10	8.51	9.06	77.9

[a] Apparent mole fraction of $AlCl_3$, excluding chloroaluminate ion formation. [b] Chloride ion mole fraction in excess of the 50 mol % $AlCl_3$-BPC melt composition. [c] The ion mole fraction of $FeCl_4^{2-}$ was identical with this. [d] Excess chloride ion less the amount complexed as $FeCl_4^{2-}$ and $FeCl_4^-$.

pra), were present in significant quantities in the basic melt.

Spectroscopic studies of iron(III) in molten alkali chlorides[17,18] generally have not provided sufficient data to permit identification of iron(III) solute species. However, Andreasen and Bjerrum[19] examined the system $FeCl_3$–$AlCl_3$–KCl at 300 °C using spectrophotometry and concluded that $FeCl_4^-$ was the principal iron(III) chloro complex in the melt when the melt pCl was 4.0 or less. Thus, the primary iron(III) species present in basic $AlCl_3$–BPC appears to be the same as that in basic inorganic chloroaluminates. These workers also reported that $FeCl_2^+$ solvated by $Al_2Cl_7^-$, $AlCl_4^-$, or Al_2Cl_6 was the most probable iron(III) species present in $AlCl_3$–KCl melt at high pCl.[19]

The stoichiometric formation constant for $FeCl_4^-$, $\beta'_{FeCl_4^-}$, can be estimated from values of $\beta'_{FeCl_4^{2-}}$ by using eq 5. A value

$$\Delta E = E^{\circ\prime}_{Fe(III)/Fe(II)} - 2.3(RT/F) \log (X_{FeCl_4^{2-}}/X_{FeCl_4^-}) - 2.3(RT/F) \log (\beta'_{FeCl_4^-}/\beta'_{FeCl_4^{2-}}) + E_j \quad (5)$$

of $E^{\circ\prime}_{Fe(III)/Fe(II)} = 2.036 \pm 0.019$ V, corrected to melt that was 66.7 mol % in $AlCl_3$, was determined for the Fe(III)/Fe(II) couple from Nernst plots obtained by coulometrically varying the ratio of iron(III) to iron(II). The slopes of these plots were 0.062 ± 0.000 V. Calculated $\beta'_{FeCl_4^-}$ values, experimental cell potentials, and ion mole fractions associated with a typical calculation involving eq 5 are presented in Table II. The estimates of $\beta'_{FeCl_4^-}$ listed in Table II were corrected for the amount of chloride ion complexed by iron(III).

The nature of the coordination of iron(III) in the 66.7 mol % $AlCl_3$–BPC melt is unknown at the present time. Attempts at obtaining meaningful UV–vis absorption spectra for iron(III) in this melt were thwarted by the UV cutoff of the melt. However, it was possible to obtain potentiometric evidence that the Fe(III)/Fe(II) half-cell reaction may be associated with at least two chloride ions in acidic $AlCl_3$–BPC melt. Figure 3 shows a plot of ΔE vs. log X_{Cl^-} for the data in Figure 2 that were acquired in acidic melt. The least-squares slope of a line through the initial portion of this curve, corresponding to data in very acidic melt, is 0.123 ± 0.005 V. A theoretical slope of 0.124 V would be expected for this plot on the basis of the half-cell reaction

$$\text{Fe(III)} + e^- \rightleftharpoons \text{Fe(II)} + 2Cl^- \quad (6)$$

One possible explanation for these results entails existence of an iron(III) species like $FeCl_2^+$ complexed or solvated by chloroaluminate ions in the acidic $AlCl_3$–BPC melt, similar to that proposed for iron(III) in acidic $AlCl_3$–KCl melt.[19] However, it should be noted that several alternate interpretations of this behavior are possible. If $FeCl_2^+$ is indeed the Fe(III) species existent in the 66.7 mol % melt, then $\beta'_{FeCl_4^-}$ would represent the product of the stepwise stoichiometric formation constants $K_3'K_4'$.

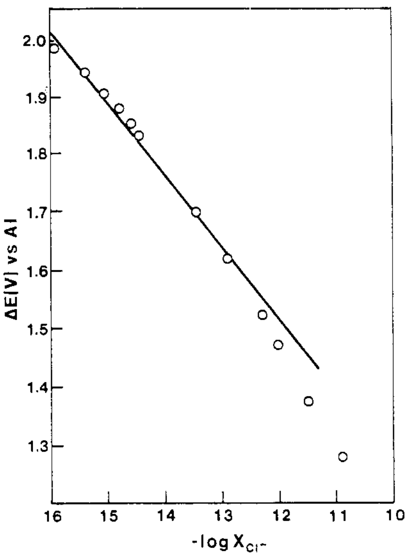

Figure 3. Dependence of the potential of the cell depicted in (II) on the chloride ion mole fraction in acidic melt at 40.0 °C. The solid line represents the calculated least-squares slope for the first eight data points.

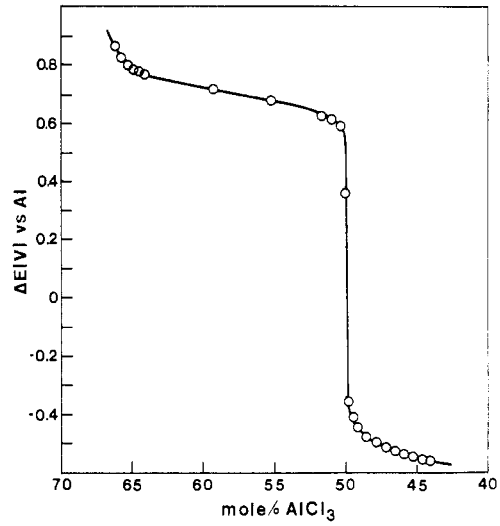

Figure 4. Potentiometric titration curve for titration of nickel(II) in $AlCl_3$–BPC at 40.0 °C. The initial nickel(II) concentration was 3.91 × 10^{-3} M. The melt was 66.3 mol % in $AlCl_3$ prior to the outset of the titration.

Nickel(II). Chloro complex equilibria involving nickel(II) were reexamined in the present study in order to obtain a value of $\beta'_{NiCl_4^{2-}}$ that was referenced to melt that was 66.7 mol % in $AlCl_3$. A representative potentiometric titration curve for nickel(II) in $AlCl_3$–BPC melt is shown in Figure 4. Insolubility of $NiCl_2$ was noted proximate to the 50.0 mol % $AlCl_3$ melt composition during a titration experiment. This effect appeared identical with that observed for $CoCl_2$[5] and $FeCl_2$ (vide supra) in $AlCl_3$–BPC but was apparently overlooked in a previous study.[4] A plot of ΔE vs. log X_{Cl^-} for the data in Figure 4 obtained in basic melt was linear with a slope of 0.134 ± 0.006 V. This slope is consistent with the formation of $NiCl_4^{2-}$ as the single nickel chloro complex in chloride ion rich melt as previously reported by Gale et al.[4] Estimates of

---

(17) Silcox, N. W.; Haendler, H. M. *J. Phys. Chem.* **1960**, *64*, 303.
(18) Harrington, G.; Sundheim, B. R. *Ann. N.Y. Acad. Sci.* **1960**, *79*, 950.
(19) Andreasen, H. A.; Bjerrum, N. J. *Inorg. Chem.* **1978**, *17*, 3605.
(20) Morrey, J. R.; Carter, D. G. *J. Chem. Eng. Data* **1968**, *13*, 94.

Table III. Potentials, Ion Mole Fractions, and Calculated Stoichiometric Formation Constants for $NiCl_4^{2-}$

E, V	X_{AlCl_3}[a]	$10^2 X_{Cl^-}$[b]	$10^4 X_{NiCl_4^{2-}}$	$10^2 X_{Cl^-}$[c]	log $\beta'_{NiCl_4^{2-}}$
−0.476	0.486	2.43	3.04	2.31	50.3
−0.495	0.479	3.77	2.95	3.65	50.1
−0.510	0.472	4.99	2.87	4.88	50.1
−0.523	0.466	6.14	2.80	6.03	50.1
−0.533	0.460	7.19	2.73	7.08	50.2
−0.524	0.453	8.23	2.67	8.12	50.2
−0.552	0.447	9.24	2.60	9.13	50.4
−0.558	0.441	10.21	2.54	10.11	50.4

[a] Apparent mole fraction of $AlCl_3$, excluding chloroaluminate ion formation. [b] Chloride ion mole fraction in excess of the 50.0 mol % $AlCl_3$–BPC melt composition. [c] Excess chloride ion less the amount complexed as $NiCl_4^{2-}$.

$\beta'_{NiCl_4^{2-}}$, referenced to nickel(II) in melt containing 66.7 mol % $AlCl_3$, were calculated from eq 7. A value of $E°'_{Ni(II)/Ni}$ = 1.017 ± 0.011 V was obtained from Nernst plots in the same fashion as was $E°'_{Fe(II)/Fe}$. This value was in good agreement with that reported by Gale et al.[4] in 60.0:40.0 mol % $AlCl_3$–BPC when the latter value was extrapolated to melt containing 66.7 mol % $AlCl_3$. Data associated with the calculation of $\beta'_{NiCl_4^{2-}}$ from the potential vs. composition data shown in Figure 4 are collected in Table III.

$$\Delta E = E°'_{Ni(II)/Ni} + 2.3(RT/2F) \log X_{NiCl_4^{2-}} - 2.3(RT/2F) \log \beta'_{NiCl_4^{2-}} - 2.3(RT/2F) \log X_{Cl^-}{}^4 + E_j \quad (7)$$

Conclusion

Average estimates of the stoichiometric chloro complex formation constants for iron(II), iron(III), and nickel(II), determined in this study, are collected in Table IV. The values reported in this table reflect the combined results of several titration experiments for each species. It is significant that cobalt(II), iron(II), iron(III), and nickel(II) all exist as mononuclear, tetrahedral complexes in the basic $AlCl_3$–BPC melt region that is accessible at 40 °C.

Table IV. Metal Ion Chloro Complexes and Average Stoichiometric Formation Constants in Chloroaluminate Melts

species	melt	t/°C	log β'	ref
$CoCl_4^{2-}$	$AlCl_3$-LiCl	300	6.5	8
	$AlCl_3$-NaCl	300	11.2	8
	$AlCl_3$-KCl	300	19.1	8
	$AlCl_3$-CsCl	400	19.7	8
	$AlCl_3$-BPC	36	46.2 ± 0.1	5
$FeCl_4^{2-}$	$AlCl_3$-BPC	40	46.6 ± 0.7	this work
$FeCl_4^-$	$AlCl_3$-KCl	300	14.8[b,c]	19
	$AlCl_3$-BPC	40	77.9 ± 0.2[b]	this work
$NiCl_4^{2-}$	$AlCl_3$-BPC	40	46.4 ± 0.8[a]	4
	$AlCl_3$-BPC	40	49.7 ± 0.5	this work

[a] Referenced to the 60.0 mol % melt. [b] Calculated on the basis of the equilibrium $FeCl_2^+ + 2Cl^- \rightleftharpoons FeCl_4^-$. [c] The p$K$ value for the reaction given above was calculated from the equilibrium constants given in ref 19. This value was then converted to a mole fraction basis by using the relationship $\log \beta' = 2 \log (n_t/V) - pK$, where n_t is the average number of moles of ions in V liters of melt. Density data for $AlCl_3$-KCl used in this calculation were taken from Morrey and Carter.[20]

There is a paucity of data concerning chloro complex equilibria in other chloroaluminate melts with which to make even qualitative comparisons with the data in Table IV. However, the magnitudes of the formation constants for all of the 3d transition-metal chloro complex ions examined thus far indicate that these complexes are exceptionally stable in basic $AlCl_3$–BPC melt. The data that are available for comparison (Table IV) suggest much greater stability of chloro complex species in the low-temperature chloroaluminate melt system vs. the higher temperature inorganic chloroaluminate melts. It is unlikely that temperature differences between these systems result in such an enormous dissimilarity in complex stability. The enhanced stability of metal chloro complexes in $AlCl_3$–BPC relative to that in the latter systems may reflect that electrostatic effects between the polarizable *N*-*n*-butylpyridinium cation and melt chloride ion are weak compared to similar effects involving the smaller alkali-metal cations found in inorganic chloroaluminate systems. Further experiments are in progress to test this supposition.

The decreased stability of $FeCl_4^{2-}$ and $CoCl_4^{2-}$, relative to that of $NiCl_4^{2-}$, in $AlCl_3$–BPC melt appears to conform to the trend predicted from the Irving–Williams series.[21] However, data obtained in the present study are not precise enough to allow meaningful comparison of the stability of $FeCl_4^{2-}$ relative to that of $CoCl_4^{2-}$ in $AlCl_3$–BPC.

Acknowledgment. Financial support for this work was provided by the National Science Foundation, Grant No. CHE-8025235.

---

(21) Cotton, F. A.; Wilkinson, G. "Advanced Inorganic Chemistry", 3rd ed.; Interscience: New York, 1972; pp 596–597.